ELSEVIER

Ceramics International 33 (2007) 905–909

CERAMICS
INTERNATIONAL

www.elsevier.com/locate/ceramint

Effects of polycarbosilane infiltration processes on the microstructure and mechanical properties of 3D-C_f/SiC composites

Ke Jian *, Zhao-Hui Chen, Qing-Song Ma,
Hai-feng Hu, Wen-Wei Zheng

Key Laboratory of Advanced Ceramic Fibers & Composites, National University of Defense Technology,
Changsha 410073, People's Republic of China

Received 7 September 2005; received in revised form 29 January 2006; accepted 20 February 2006

Abstract

Three-dimensional braided carbon fiber-reinforced silicon carbide (3D-C_f/SiC) composites were prepared through eight cycles of infiltration of polycarbosilane (PCS)/divinylbenzene (DVB) and subsequent pyrolysis under an inert atmosphere. The effects of infiltration processes on the microstructure and mechanical properties of the C_f/SiC composites were investigated. The results showed that increasing temperature could reduce the viscosity of the PCS/DVB solution, which was propitious to the infiltration processes. The density and flexural strength of 3D-C_f/SiC composites fabricated with vacuum infiltration were 1.794 g cm^{-3} and 557 MPa, respectively. Compared to vacuum infiltration, heating and pressure infiltration could improve the infiltration efficiency so that the composites exhibited higher density and flexural strength, i.e., 1.944 g cm^{-3} and 662 MPa. When tested at 1650 °C and 1800 °C in vacuum, the flexural strength reached 647 MPa and 602 MPa, respectively.

Keywords: B. Interfaces; Infiltration processes; Density; Viscosity; C_f/SiC composites

---

1. Introduction

C_f/SiC materials benefit from the high-temperature capability of carbon fibers and high modulus and oxidation resistance of the SiC matrix [1]. As a fiber-reinforced composite, the mechanical and thermal properties can be tailored by adjusting fiber volume and placement to meet the needs of many applications. Additional flexibility can be achieved with the wide variety of carbon fibers available for reinforcement. Silicon carbide has good high-temperature strength that is maintained to around 1700 °C, sufficient thermal shock resistance, a low thermal expansion coefficient, and good thermal conductivity [2]. As a result, C_f/SiC composites are considered as desirable high-temperature structural materials and have wide application in various fields.

There are several methods to fabricate C_f/SiC composites, such as chemical vapor infiltration (CVI), slurry infiltration combined with hot-pressing and polymer-infiltration-pyrolysis (PIP), etc. [3–5]. Of these methods, the PIP route is being actively developed because it offers many potential advantages such as low processing temperature, controllable ceramic compositions, and near-net-shape technologies.

The mechanical properties of C_f/SiC composites are determined by their microstructures. It is well demonstrated that weak interfacial bonding and high densities are preferred in order to obtain high performance C_f/SiC composites [6,7]. The microstructures of C_f/SiC composites are governed by the fabrication process. The manufacturing of C_f/SiC composites via PIP includes three stages. In stage 1, the fiber preform is infiltrated with precursor solution. In stage 2, the precursor is cured into a solid. In stage 3, the cured solid is pyrolyzed in an inert or reactive atmosphere. Several infiltration-cure-pyrolysis cycles are required to densify composites because evolution of gaseous products and volume shrinkage occur during pyrolysis, resulting in micro-cracks and pores in the matrix. The influence of the pyrolysis processes have been discussed in detail in previous papers [8,9], but there are still relatively few reports about the effects of the different infiltration processes on mechanical properties and microstructure of C_f/SiC prepared by PIP route.

---

* Corresponding author.
E-mail address: jianke_nudt@sina.com (K. Jian).

doi:10.1016/j.ceramint.2006.02.005

In this paper, carbon fiber-reinforced silicon carbide composites were fabricated with polycarbosilane (PCS) and divinylbenzene (DVB) as precursors, and the effects of the infiltration processes on the microstructure and mechanical properties of 3D-C_f/SiC composites were investigated.

2. Experimental procedure

2.1. Raw materials

Three-dimensional braided carbon fiber (3D-C_f) was used as the reinforcement. It was two-step braided in Nanjing Fiberglass Research & Design Institute. Fiber volume fraction in x, y, z directions of three-dimensional braided carbon fiber preform was 8:1:1. The fibers were Jitan fibers (Jilin Carbon Corp., China) and the tensile strength and elastic modulus of them were about 3000 MPa and 210 GPa, respectively.

Polycarbosilane whose average molecular weight and softening point were about 1300 and 210 °C was used as the precursor to SiC ceramics. It was synthesized by ourselves. Divinylbenzene was used as solvent and cross-linking reagent for PCS. In previous work, the PCS/DVB solution with a mass ratio of 1:0.4 was demonstrated to be proper to prepare C_f/SiC composites [10].

2.2. Preparation of 3D-B C_f/SiC

Two samples which were denoted as 3D-VI and 3D-PI were prepared with different infiltration processes. First, the 3D carbon fiber preforms were put into an airtight vessel, and then the preforms were infiltrated with PCS/DVB solution in vacuum conditions. Then the 3D-VI was put into the oven directly and heated to 150 °C. The temperature was maintained for about 6 h to ensure PCS/DVB solution to cure into a solid. On the other hand, 3D-PI was diverted into an autoclave and heated to 80 °C, and then 6 MPa nitrogen atmosphere was purged. About 60 min later, the autoclave was heated to 150 °C and left at this temperature for about 6 h. Afterwards, the cured 3D-VI and 3D-PI were pyrolyzed at high temperature in an inert atmosphere. To densify the composites, seven infiltration-cure-pyrolysis cycles were repeated in the same conditions as those of the initial cycle.

2.3. Characterization of the composites

The viscosities of the PCS/DVB solution were tested with a calibrated Ubbelohde-type capillary viscometer.

The bulk densities of the composites were computed from the weight-to-volume ratio.

Three-point bending tests were used to evaluate flexural strength of the composites with the span/height ratio of 15 and a crosshead speed of 0.5 mm/min. The flexural strength of composites at room temperature was tested at Central South University, China, using a universal testing machine (Instron-1342). The flexural strength of composites at high temperature in vacuum was tested at Northwestern Polytechnical University, China, using a flexural and tensile testing machine (YKM-2200). For the mechanical properties test, three 3 mm × 4 mm × 70 mm specimens were measured for each composite. The load–displacement curves were recorded simultaneously by using load-cell and laser extensometer. The elastic modulus of the composites were measured from the slope of the linear portion of the load–displacement curves.

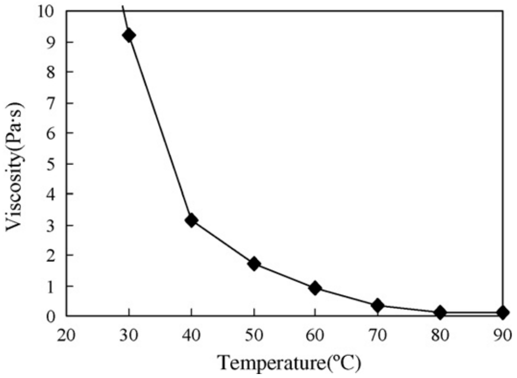

Fig. 1. Viscosity–temperature curve of PCS/DVB solution.

Fracture surfaces of the specimens after three-point bending tests were examined by scanning electron microscopy (SEM).

3. Results and discussion

3.1. The influence of temperatures on the viscosity of the PCS/DVB solution

In a previous work, the PCS/DVB solution with a mass ratio of 1:0.4 was demonstrated to be proper to prepare C_f/SiC composites. Nevertheless, the solution had high viscosity at room temperature resulting in a great difficulty to impregnate the solution into the carbon fiber preforms. The viscosity depends on the temperature are shown in Fig. 1. When the temperature was increased to 80 °C, the viscosity of the solution reduced to 0.104 Pa s and it exhibited a good flowability. Nevertheless with a temperature above 80 °C, the solution will cure rapidly which is greatly disadvantageous to the infiltrative processes.

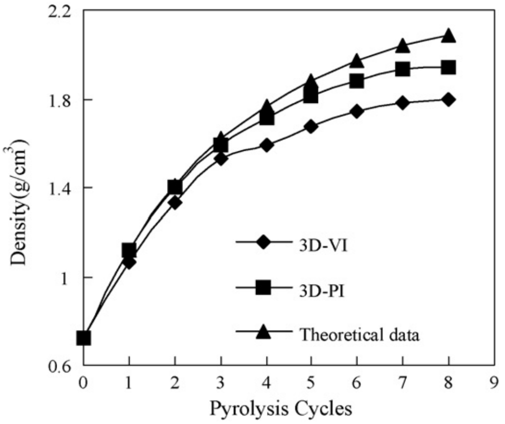

Fig. 2. Density–infiltration time curves of 3D-C_f/SiC.

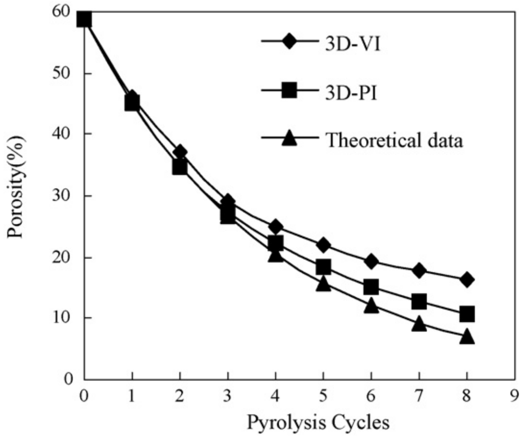

Fig. 3. Porosity–infiltration time curves of 3D-C_f/SiC.

3.2. The influence of infiltration processes on the densities and porosities of the C_f/SiC composites

According to the viscosity–temperature curve, the parameters of the heating and pressure infiltration to fabricate 3D-PI were determined. In order to make a comparison, 3D-VI was fabricated by vacuum infiltration.

Density is one of the most important factors for the mechanical properties of the C_f/SiC composites. The experimental and theoretical densities and porosities of the samples in relation to the number of cycles are shown in Figs. 2 and 3, respectively. In Figs. 2 and 3, ρ_0 and θ_0 are the density and porosity of the 3D-C_f preforms. In this case, ρ_0 and θ_0 are given by

$$\rho_0 = \frac{m_f}{V_0} \tag{1}$$

$$\theta_0 = 1 - \frac{\rho_0}{\rho_f} \tag{2}$$

where m_f is the mass of the carbon fiber performs; V_0, the volume of the carbon fiber performs; and ρ_0, the density of the carbon fiber (about 1.76 g cm^{-3}).

The experimental densities of the composites were computed from the weight-to-volume ratio and the experimental porosities were obtained from

$$\rho_n^E = \frac{m_n^E}{V} \quad (n \geq 1) \tag{3}$$

$$\theta_n^E = \theta_{n-1}^E - \frac{m_n^E - m_{n-1}^E}{V\rho_{Si-C}} \quad (n \geq 1) \tag{4}$$

where the superscript E means experimental data and the subscript denotes the number of the fabrication cycles; m, the mass of the C/SiC composites; ρ_{Si-C}, the density of PCS/DVB solution and SiC matrix derived from PCS/DVB pyrolysis (about 2.55 g cm^{-3}); and V, the volume of the composites. Because the volume of the composites changes slightly, V is used to denote the volume of the composites during the whole fabrication processes.

The theoretical densities and porosities are given by

$$\rho_n^T = \rho_{n-1}^T + \theta_{n-1}^T \eta \rho_{PCS/DVB} \quad (n \geq 1) \tag{5}$$

$$\theta_n^T = \theta_{n-1}^T - \frac{\theta_{n-1}^T \eta \rho_{PCS/DVB}}{\rho_{Si-C}} \quad (n \geq 1) \tag{6}$$

where the superscript T means theoretical data; $\rho_{PCS/DVB}$, the density of PCS/DVB solution (about 1.02 g cm^{-3}); and η, the ceramic yield of the cured PCS/DVB (about 0.58).

Figs. 2 and 3 clearly show that the density–number of cycles curve of the 3D-PI was closer to the theoretical curve than that of the 3D-VI, i.e., the density of 3D-PI was increased much faster than for 3D-VI, i.e., compared to vacuum infiltration, heating and pressure infiltration could improve the infiltration efficiency.

3.3. The influence of infiltration processes on the flexural strength of the C_f/SiC composites

The properties of the C_f/SiC composites fabricated with different infiltration processes are shown in Table 1. The density and flexural strength of 3D-VI were 1.794 g cm^{-3} and

Table 1
Properties of 3D-C_f/SiC composites fabricated by different infiltration processes

Sample	Density (g cm^{-3})	Porosity (%)	Flexural strength (MPa)
3D-VI	1.794	16.48	557
3D-PI	1.944	10.60	662

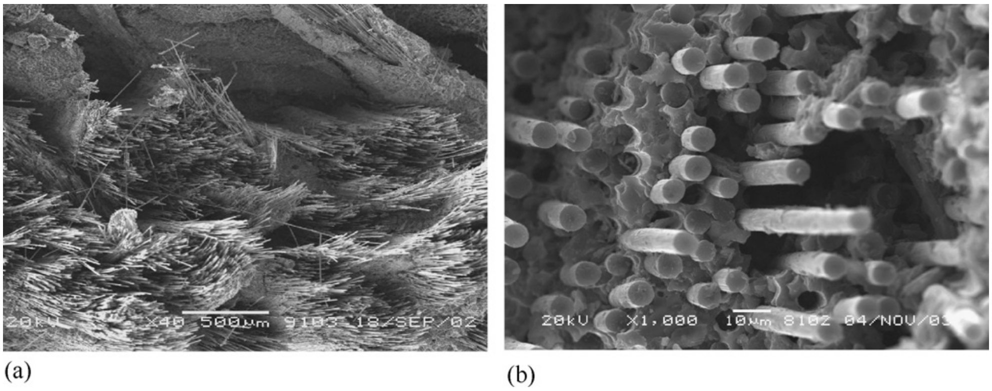

Fig. 4. SEM photos of fracture surface of the 3D-VI composites. (a) Sample 3D-VI (×40) and (b) sample 3D-VI (×1000).

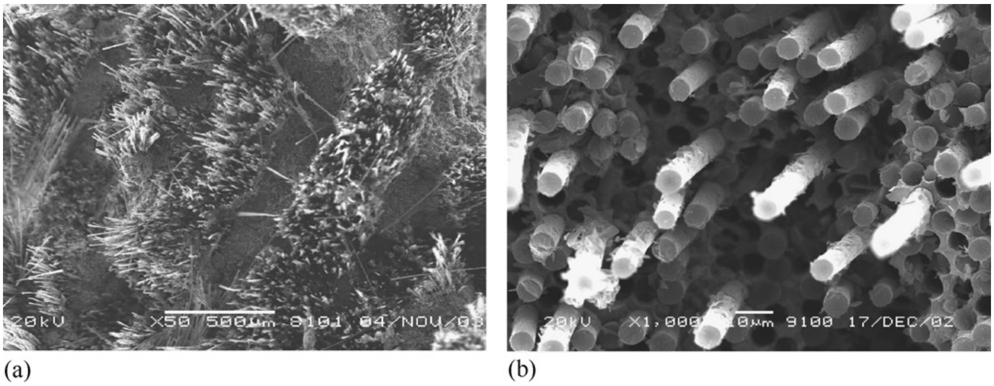

(a) (b)

Fig. 5. SEM photos of fracture surface of the 3D-PI composites. (a) Sample 3D-PI (×50) and (b) sample 3D-PI (×1000).

557 MPa, respectively. The 3D-PI composites exhibited higher density and flexural strength, 1.944 g cm^{-3} and 662 MPa, respectively.

The fracture surfaces of the 3D-VI and 3D-PI composites are given in Figs. 4 and 5. Both kinds of composites show an extensive fiber-debonding and pull-out, which indicates a relatively weak fiber/matrix interfacial bonding. It was well demonstrated that weak interfacial bonding could result in high mechanical properties. As a result, 3D-VI and 3D-PI also exhibited high flexural strength. At the same time it could be observed that the number and length of the pull-out fibers of the composites were similar for the 3D-VI and 3D-PI composites. Consequently, the difference of the flexural strength did not result from different interfacial structures.

Density is another important factor to affect the mechanical properties of the C_f/SiC composites. Fig. 4 shows that in the 3D-VI composites, big sized pores exist within the fasciculi and many small sized pores exist among the fibers. Pores derive from (i) the evolution of gaseous products occurring during PCS/DVB pyrolysis, (ii) the incomplete infiltration of the precursor solution, and (iii) the difference of the coefficient of thermal expansion between carbon fiber and SiC matrix. Fig. 5 shows that the number and size of the pores in the 3D-PI composites decrease markedly compared to the 3D-VI composites. By the heating and pressure infiltration processes, the PCS/DVB solution could be impregnated into the pores more easily than for vacuum infiltration. As a result, compared to vacuum infiltration, heating and pressure infiltration could improve the infiltration efficiency so that the 3D-PI had higher density, which agrees with the results of Fig. 2. Therefore, 3D-PI exhibited higher flexural strength than 3D-VI.

3.4. Mechanical properties of C_f/SiC at high temperature

The flexural strength of the 3D-PI composites tested at different temperatures in vacuum is shown in Table 2. The flexural strength show a slight decrease when tested at 1650 °C and 1800 °C, the residual strength being 97.7% and 92.0%, respectively. On the contrary, the flexural modulus reduced greatly at high temperature, the residual flexural modulus being only 48.6% and 25.0%, respectively. The decrease in the flexural modulus at high temperature is mainly to be attributed to the softening of the SiC matrix.

Table 2
Mechanical properties of 3D-C_f/SiC at high temperatures

Tested temperature (°C)	Flexural strength (MPa)	Flexural modulus (GPa)
20	662	131
1650	647	63.7
1800	609	32.8

4. Conclusions

(1) With the increase of temperature, the viscosity of the PCS/DVB solution reduced sharply. Nevertheless with too high temperatures, the solution would cure in a too short time. 80 °C was a proper temperature for the impregnation of PCS/DVB solution.

(2) The density and flexural strength of the composites fabricated with vacuum infiltration were only 1.794 g cm^{-3} and 557 MPa, respectively. The composites fabricated with heating and pressure infiltration exhibited higher density and flexural strength, 1.944 g cm^{-3} and 662 MPa, respectively. Both composites exhibited a weak fiber-matrix interfacial bonding and the difference of the strength did not result from the different interfacial structures. The increase of the flexural strength was mainly attributed to the decrease of the porosity that resulted from the improvement of the infiltration efficiency.

(3) Tested at 1650 °C and 1800 °C in vacuum, the flexural strength reached 647 MPa and 602 MPa, respectively. The 3D-C_f/SiC composites exhibited good flexural strength at high temperatures. Nevertheless, the residual flexural modulus was only 48.6% and 25.0% at 1650 °C and 1800 °C, respectively. The decrease in the flexural modulus at high temperature was mainly attributed to the softening of the SiC matrix.

References

[1] C. Thomas, T. Joseph, A. Peter, M. James, Ceram. Eng. Sci. Proc. 21 (3) (2000) 517–524.

[2] S.M. Zhu, S.Q. Ding, H.A. Xi, R.D. Wang, Mater. Lett. 59 (5) (2005) 595–597.
[3] J. Suo, Z.H. Chen, J.Y. Xiao, W.W. Zheng, Ceram. Int. 31 (2005) 447–452.
[4] M.Z. Berbon, D.R. Dietrith, D.B. Marshall, J. Am. Ceram. Soc. 84 (10) (2001) 2229–2234.
[5] T. Noda, H. Araki, H. Suzuki, J. Nucl. Mater. 212–1 (9) (1994) 823–829.
[6] J.F. Desprec, M. Monthioux, J. Eur. Ceram. Soc. 15 (3) (1995) 209–224.
[7] H.Q. Ly, R. Taylor, R.J. Day, J. Mater. Sci. 36 (15) (2001) 4027–4035.
[8] Z.H. Ke Jian, Q. Chen, S. Ma, W.W. Zheng, Mater. Sci. Eng. A390 (1–2) (2005) 154–158.
[9] Q.S. Ma, Z.H. Chen, W.W. Zheng, H.F. Hu, Ceram. Int. 31 (2005) 305–314.
[10] B. Su, X.J. Wu, Z.H. Chen, Polymer. Mater. Sci. Eng. 10 (2) (1994) 121–123 (in Chinese).